2.14. Statistical analysis

Data were expressed as mean ± standard error (S.E.). Comparisons of parameters among groups were made by one-way ANOVA, followed by Newman–Keuls' test. Differences were considered significant at $P<0.05$.

3. Results

3.1. Improvement in cardiac function by MSC transplantation

Two of 15 rats in the MyoC group died on day 19 and day 21 post-myosin injection, respectively, whereas the MyoC+MSC group had no mortality. At 3 weeks post-myosin injection, the MyoC group showed increased heart weight/body weight ratio (HW/BW) and LVEDP, and decreased MAP and Max d*P*/d*t* compared with the Sham group, indicating the presence of acute heart failure in this model (Fig. 1 and Table 1). These parameters subsequently returned to baseline with MSC transplantation (MyoC+MSC group). On echocardiography, the MyoC group showed an increase in LVDs and LVDd, and a significant reduction in %FS and EF (Fig. 2 and Table 2). MSC transplantation significantly improved these parameters (MyoC+MSC group).

3.2. Attenuation of myocardial inflammation by MSC transplantation

Myocardial necrosis and tissue granulation as well as giant cell infiltration and edema were markedly increased in our model of acute myocarditis (Fig. 3A). MSC transplantation significantly attenuated these changes observed in the MyoC group. MSC-transplanted hearts exhibited a consistent tendency for a reduction of tissue granulation, inflammation and edema, on blinded histological grading by a cardiovascular pathologist (H.I-U.), as compared to the MyoC group (Fig. 3B). Hearts showed limited fibrosis in the MyoC group, and this observation was not significantly attenuated by MSC

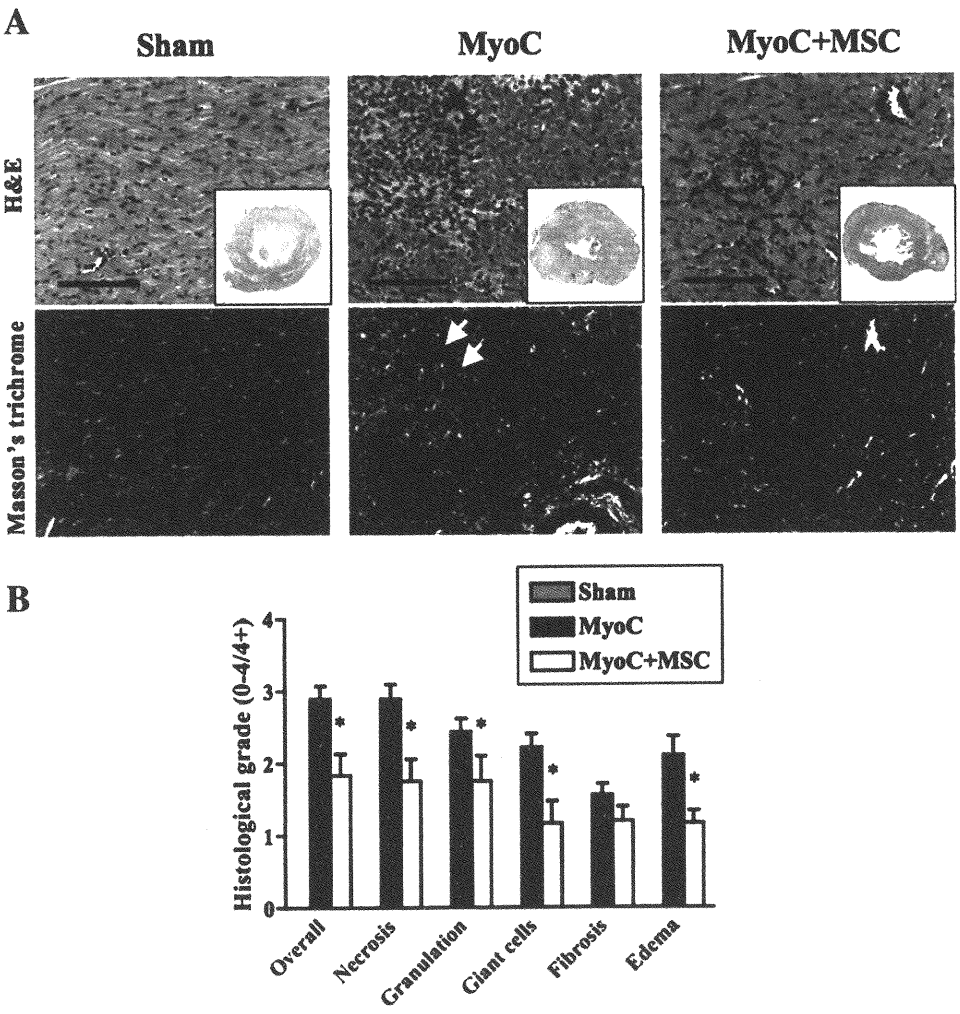

Fig. 3. Effects of MSC transplantation on pathological changes in acute myocarditis. (A) Representative myocardial sections show markedly decreased inflammation and tissue necrosis (H & E) and a comparable degree of early fibrosis (Masson's trichrome) after MSC transplantation (MyoC+MSC) as compared to control (MyoC, arrows). Insets are transverse sections of myocardium. Scale bars: 50 μm. (B) Semi-quantitative histological grades for necrosis and tissue granulation as well as for infiltration of giant cells and edema were significantly lower after MSC transplantation (MyoC+MSC) compared to control (MyoC). Sham tissues exhibited no measurable pathological change. Values are mean±S.E. *$P<0.05$ *vs* Sham, $^{\dagger}P<0.05$ *vs* MyoC group.

transplantation, possibly because of the acute nature of this experiment (Fig. 3B).

Notably, marked histiocytic infiltration was demonstrated by CD68-positive cells, including multinucleated giant cells, in myocarditis (MyoC group), and this was significantly attenuated by MSC transplantation (Figs. 4A and B). In myocarditis, there was an increase in MCP-1 expression localized to the vascular endothelium and also in cardiomyocytes surrounding areas of inflammation (Fig. 5A). The hearts in the MyoC+MSC group showed a partial decrease in MCP-1 expression. Serum MCP-1 level was greatly increased in the MyoC group, whereas the increase was significantly attenuated in the MyoC+MSC group (Fig. 5B).

3.3. Effect of MSC on angiogenesis

To investigate the angiogenic effect of MSC transplantation in the myocardium, immunohistochemical analysis of vWF was performed. Capillary density was increased in the MyoC group (Figs. 6A and B). Notably, in MSC-transplanted tissues, capillary density was increased compared to that in the MyoC group. The clustering of relatively small vessels seen in MSC-transplanted hearts was indicative of recent neovascularization.

3.4. Cardioprotective effects of MSC in paracrine manner

Because MSC transplantation had anti-inflammatory and tissue-protective effects and induced angiogenesis, some paracrine effects were expected. To confirm the paracrine effects of MSC *in vitro*, cardiomycytes were isolated from adult rats, and cultured with MCP-1 in the standard medium or in the conditioned medium obtained from MSC culture. The standard medium containing MCP-1 resulted in a decrease in viable cardiomyocytes; however, MSC-derived conditioned medium containing MCP-1 attenuated the decrease in viable cardiomyocytes (Fig. 7A). TUNEL staining showed that the standard medium containing MCP-1 markedly induced apoptosis of cardiomyocytes (Figs. 7B and C). However, the conditioned medium of MSC significantly attenuated MCP-1-induced cardiomyocyte apoptosis. In addition, CK activity in standard medium containing MCP-1 was significantly increased, whereas the conditioned medium markedly attenuated the CK activity induced by MCP-1 (Fig. 7D).

To investigate whether MSC secreted angiogenic and anti-fibrotic factors, VEGF and HGF levels in MSC culture were measured by ELISA assay. MSC secreted large amounts of VEGF and HGF compared to standard medium, respectively (Fig. 7E).

4. Discussion

In this study, we focused on the therapeutic potential of MSC transplantation in the acute phase of myocarditis. We showed that 1) MSC transplantation 1 week after myosin injection improved cardiac function and attenuated pathological findings including myocardial inflammation, and that 2)

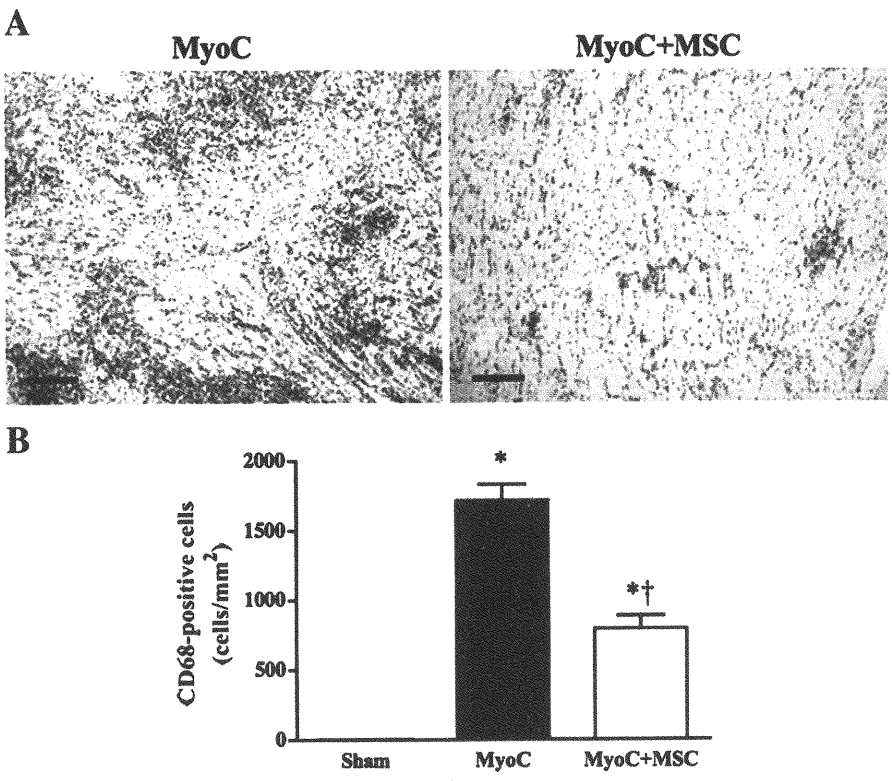

Fig. 4. Effects of MSC transplantation on myocardial CD68 expression in acute myocarditis. (A) Representative myocardial sections immunohistochemically stained for CD68 demonstrate a marked decrease in CD68-positive cells, including giant cells, after MSC transplantation (MyoC+MSC) as compared to control (MyoC). Scale bars: 100 μm. (B) Semi-quantitative counts of CD68-positive cells demonstrate a significant reduction in the MyoC+MSC group. Values are mean±S.E. $^{*}P<0.05$ *vs* Sham, $^{\dagger}P<0.05$ *vs* MyoC group.

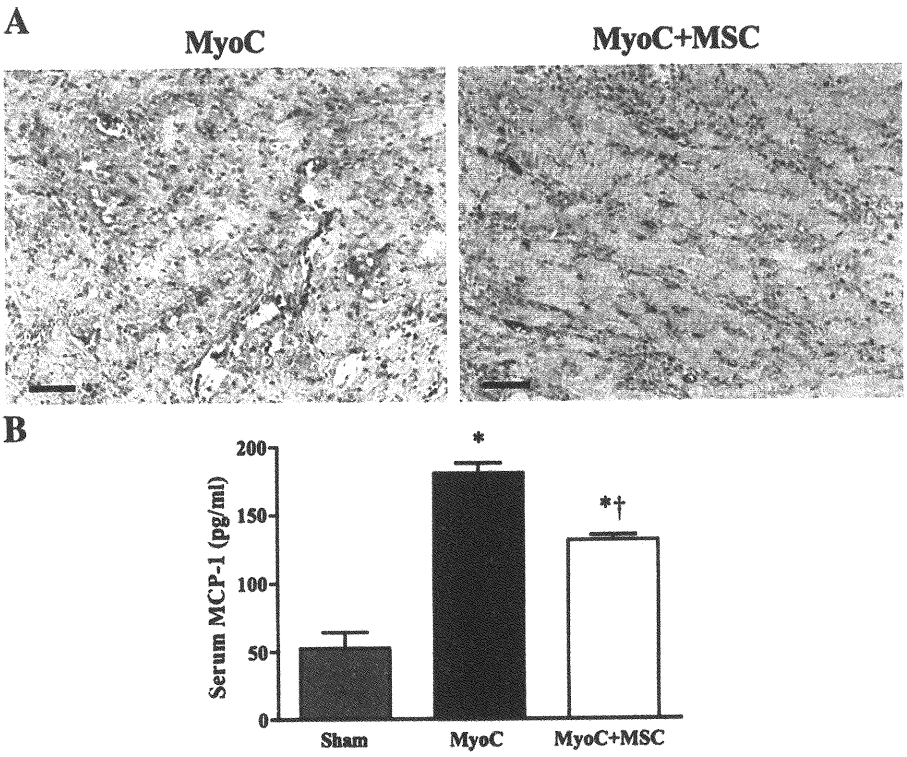

Fig. 5. Effects of MSC transplantation on myocardial MCP-1 expression and serum MCP-1 level. (A) Representative MCP-1-stained myocardial sections from MyoC and MyoC+MSC groups. Scale bars: 50 μm. (B) Serum level of MCP-1 measured by ELISA. Values are mean±S.E. *$P<0.05$ *vs* Sham, †$P<0.05$ *vs* MyoC group.

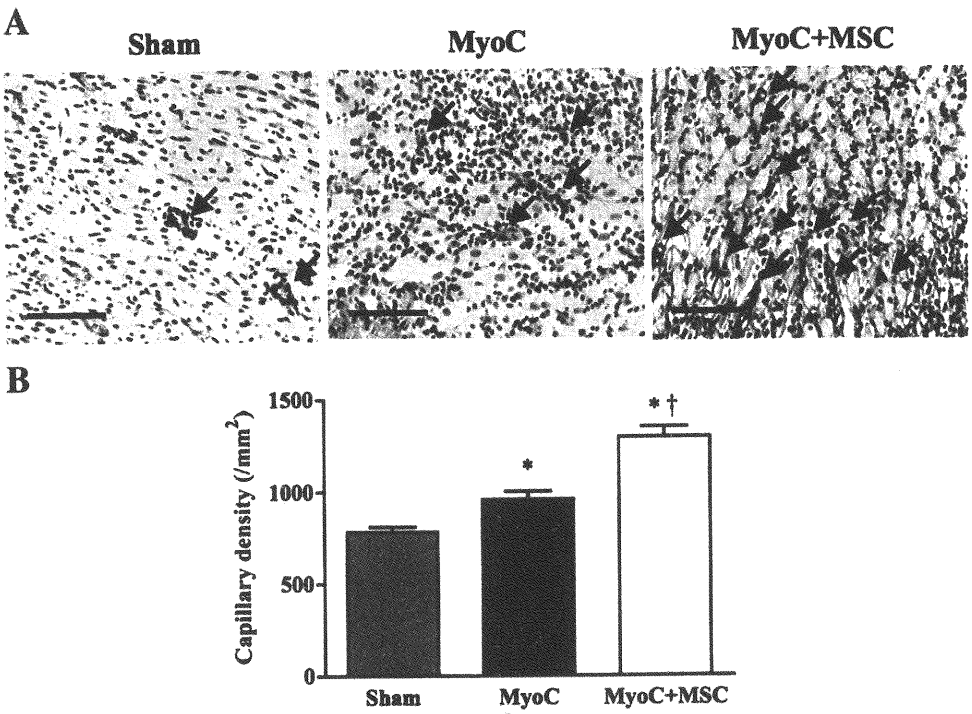

Fig. 6. Effects of MSC on neovascularization. (A) Representative myocardial sections immunohistochemically stained for vWF showing increased microvasculature (arrows) in control hearts (MyoC), which was more marked after MSC transplantation (MyoC+MSC). Scale bars: 50 μm. (B) Capillary density measured in 10 random representative high-power fields showing a significant increase in control (MyoC) and a further increase after MSC transplantation (MyoC+MSC) over the Sham group. Values are mean±S.E. *$P<0.05$ *vs* Sham, †$P<0.05$ *vs* MyoC group.

MSC had cardioprotective effects acting in a paracrine manner.

The rat model of myosin-induced experimental myocarditis provides a model that resembles human giant cell myocarditis [8,10]. Although the majority of acute myocarditis is linked to a viral infection such as coxsackievirus B3, this viral infection can in some cases cause an autoimmune myocarditis with chronic myocardial inflammation without viral persistence, due to the exposure of cardiac autoantigens to the immune system [11,12]. This myocarditis model is triphasic, consisting of an antigen priming phase from days 0–14, an autoimmune response phase from days 14–21, and a reparative phase thereafter, associated chronically with a dilated cardiomyopathy phenotype [13]. In our previous study, MSC were transplanted at the reparative

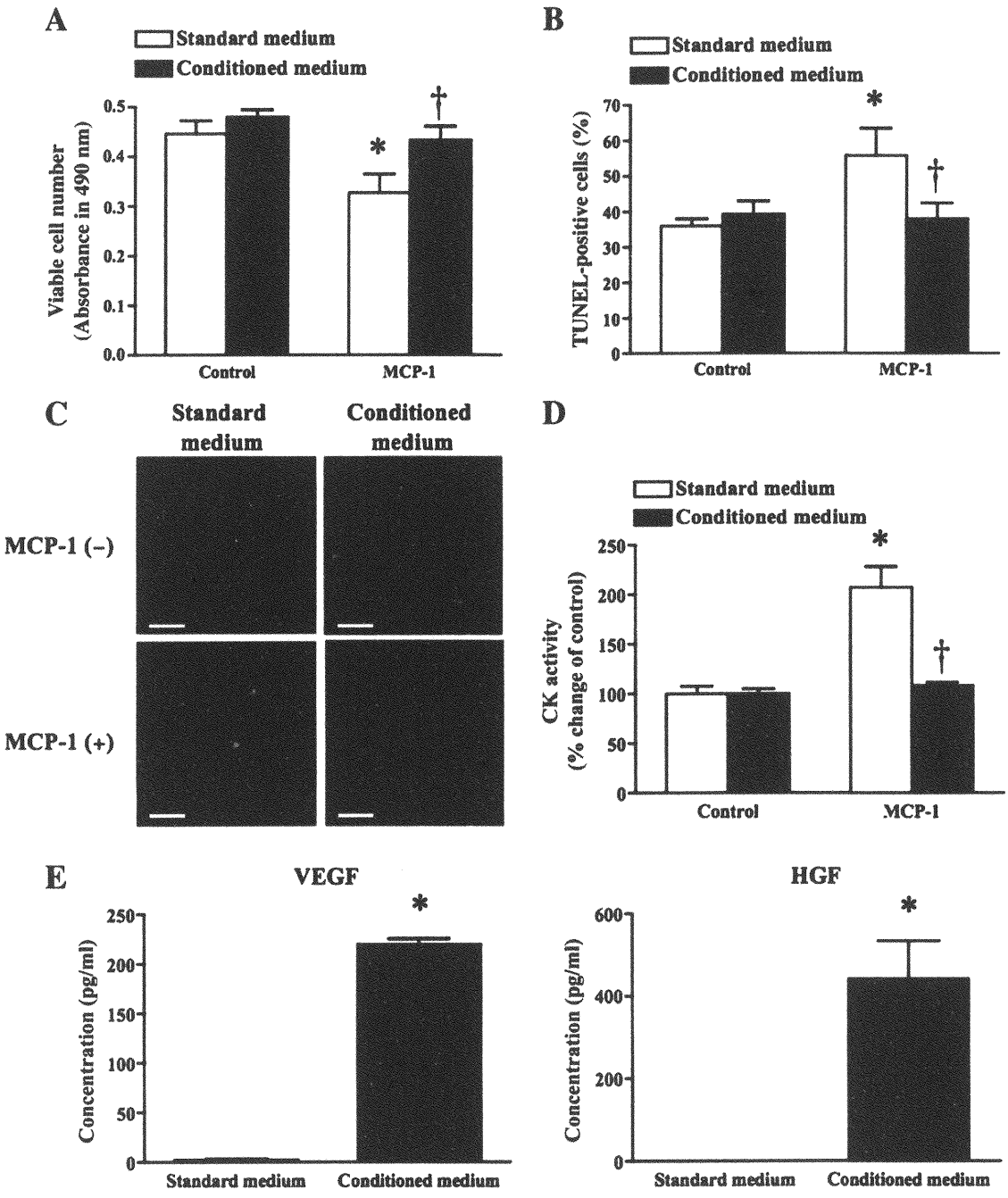

Fig. 7. Effects of MSC on MCP-1-induced cardiomyocyte injury *in vitro*. (A) MTS assay after 24 h of culture with or without MCP-1 in standard medium *vs* MSC conditioned medium. $^{*}P<0.05$ *vs* control in standard medium, $^{\dagger}P<0.05$ *vs* MCP-1 in conditioned medium. (B) Quantitative analysis of TUNEL staining after 24 h of culture with or without MCP-1 in standard medium *vs* MSC conditioned medium. $^{*}P<0.05$ *vs* control in standard medium, $^{\dagger}P<0.05$ *vs* MCP-1 in standard medium. (C) Representative TUNEL staining show increased apoptotic cardiomyocytes (green) cultured with MCP-1 in standard medium, which was attenuated by MSC conditioned medium. Nuclei were counterstained with DAPI (blue). Scale bars: 50 μm. (D) CK activity after 24 h of culture with or without MCP-1 in standard medium *vs* MSC conditioned medium. $^{*}P<0.05$ *vs* control in standard medium, $^{\dagger}P<0.05$ *vs* MCP-1 in standard medium. (E) ELISA for VEGF and HGF secreted from cultured MSC as compared to standard medium. $^{\dagger}P<0.05$ *vs* standard medium.

phase with a dilated cardiomyopathy phenotype, by direct injection into the myocardium [7]. In the present study, however, MSC were transplanted 1 week following myosin injection, corresponding to the acute phase of myocarditis, by intravenous injection, because this model is more relevant to clinical situations. Myosin injection caused acute heart failure as indicated by increased LVEDP and decreased Max d*P*/d*t* and %FS, and 2 out of 15 rats died; however, intravenous injection of MSC in the acute phase significantly improved the heart failure as determined by improvement of these parameters, and no death was observed.

Wang et al. have shown that embryonic stem (ES) cells transplanted into a mouse model of myocarditis regenerate cardiomyocytes, decrease inflammation and increase survival, possibly through migration of ES cells and differentiation into cardiomyocytes [14]. In the present study, we examined the therapeutic potential of transplanted MSC, which are more applicable to clinical situations than ES cells, in a rat model of acute myocarditis. Recent studies have demonstrated that autologous or allogeneic MSC strongly suppress T-lymphocyte proliferation [15,16]. These findings raise the possibility that MSC have the ability to attenuate inflammatory responses. Interestingly, the present study demonstrated that transplantation of MSC attenuated the infiltration of CD68-positive inflammatory cells and the expression of MCP-1 in a rat model of acute myocarditis. MCP-1 is a member of the C–C subfamily of chemokines with chemoattractant activity for major inflammatory cells, and is known to play an important role in the induction of experimental acute myocarditis [17,18]. Cardiac-targeted expression of MCP-1 results in monocyte/macrophage infiltration into the heart, and causes interstitial fibrosis and ventricular chamber dilation [19]. In the myosin-induced acute myocarditis model, MCP-1 expression is increased in the heart from days 15–27 post-myosin injection, and serum MCP-1 level is elevated from days 15–24 [18]. In consistent with this report, our model showed an increase in MCP-1 in the heart and serum on day 21 post-myosin injection, and MSC transplantation attenuated the increase in MCP-1 and the infiltration of CD68-positive inflammatory cells. Furthermore, earlier studies have shown that MSC express CCR2, the receptor for MCP-1, and that MCP-1 promotes the migration of MSC that express CCR2 [20,21]. Thus, it is speculated that MSC secrete some anti-inflammatory factors in response to MCP-1; however, the precise mechanisms for the anti-inflammatory effect still remains to be elucidated.

Because MCP-1 plays an important role in this myosin-induced myocarditis model, we examined the direct effect of MCP-1, besides its chemoattractant activity, on adult rat cardiomyocytes. Our *in vitro* experiment demonstrated that MCP-1 stimulation on cardiomyocytes resulted in an increase of cell injury and death, whereas MSC-derived conditioned medium attenuated these effects. It has been reported that CCR2 expression is increased in the failing myocardium, and MCP-1 stimulation on cardiomyocytes induces other inflammatory cytokines such as IL-1β and IL-6, which may reduce cardiomyocyte contractility partly via induction of apoptosis [22–25]. In addition, our previous and present study demonstrated that cultured MSC secreted large amounts of angiogenic and anti-apoptotic factors such as VEGF, HGF, insulin-like growth factor-1 and adrenomedullin [7]. Furthermore, a recent study demonstrated that conditioned medium obtained from MSC culture had cardioprotective effect [26]. Taken together, although various factors might be involved, MSC might have cardioprotective effects in a paracrine manner in response to MCP-1.

In the present study, MSC transplantation increased capillary density in the myocardium. Improvement in myocardial vascular supply has been shown to decrease necrosis and inflammation in viral myocarditis [8,27,28]. We have previously reported increased capillary density associated with improved cardiac function and decreased infarct size following MSC transplantation in a rat model of myocardial infarction [5]. These results suggest that MSC-induced neovascularization may have contributed to the improvement of cardiac function in this rat model of acute myocarditis. However, when PKH26 dye-labeled MSC were intravenously injected in rats with acute myocarditis, only a small fraction of PKH26-labeled cells were positive for troponin T 2 weeks after transplantation (data not shown). Our previous study demonstrated that ~3% of the intravenously administered MSCs were incorporated into the heart 24 h after transplantation in rats with acute myocardial infarction [5]. Although the animal model and the evaluation time were different, our present study showed that only a small number of administered MSC was differentiated into endothelial cells or cardiomyocytes, thus the contribution of the differentiated MSC to the improvement of cardiac function in this model appears to be rather insignificant.

In conclusion, MSC transplantation attenuated myocardial injury and dysfunction in a rat model of acute myocarditis, at least in part through paracrine effects of MSC.

Acknowledgments

This work was funded by a post-doctoral fellowship from the Japan Society for the Promotion of Science, and research grants for Cardiovascular Disease (16C-6, 17C-1 and 18C-1) and Human Genome Tissue Engineering 009 from the Ministry of Health, Labor and Welfare.

References

[1] Levi D, Alejos J. Diagnosis and treatment of pediatric viral myocarditis. Curr Opin Cardiol 2001;16:77–83.
[2] Feldman AM, McNamara D. Myocarditis. N Engl J Med 2000;343:1388–98.
[3] Pittenger MF, Mackay AM, Beck SC, Jaiswal RK, Douglas R, Mosca JD, et al. Multilineage potential of adult human mesenchymal stem cells. Science 1999;284:143–7.
[4] Le Blanc K, Pittenger M. Mesenchymal stem cells: progress toward promise. Cytotherapy 2005;7:36–45.
[5] Nagaya N, Fujii T, Iwase T, Ohgushi H, Itoh T, Uematsu M, et al. Intravenous administration of mesenchymal stem cells improves cardiac function in rats with acute myocardial infarction through angiogenesis and myogenesis. Am J Physiol: Heart Circ Physiol 2004;287:H2670–6.

[6] Miyahara Y, Nagaya N, Kataoka M, Yanagawa B, Tanaka K, Hao H, et al. Monolayered mesenchymal stem cells repair scarred myocardium after myocardial infarction. Nat Med 2006;12:459–65.
[7] Nagaya N, Kangawa K, Itoh T, Iwase T, Murakami S, Miyahara Y, et al. Transplantation of mesenchymal stem cells improves cardiac function in a rat model of dilated cardiomyopathy. Circulation 2005; 112:1128–35.
[8] Kodama M, Matsumoto Y, Fujiwara M, Masani F, Izumi T, Shibata A. A novel experimental model of giant cell myocarditis induced in rats by immunization with cardiac myosin fraction. Clin Immunol Immunopathol 1990;57:250–62.
[9] Tanaka K, Honda M, Takabatake T. Redox regulation of MAPK pathways and cardiac hypertrophy in adult rat cardiac myocyte. J Am Coll Cardiol 2001;37:676–85.
[10] Kodama M, Matsumoto Y, Fujiwara M, Zhang SS, Hanawa H, Itoh E, et al. Characteristics of giant cells and factors related to the formation of giant cells in myocarditis. Circ Res 1991;69:1042–50.
[11] Fairweather D, Kaya Z, Shellam GR, Lawson CM, Rose NR. From infection to autoimmunity. J Autoimmun 2001;16:175–86.
[12] Cunningham MW. T cell mimicry in inflammatory heart disease. Mol Immunol 2004;40:1121–7.
[13] Kodama M, Hanawa H, Saeki M, Hosono H, Inomata T, Suzuki K, et al. Rat dilated cardiomyopathy after autoimmune giant cell myocarditis. Circ Res 1994;75:278–84.
[14] Wang JF, Yang Y, Wang G, Min J, Sullivan MF, Ping P, et al. Embryonic stem cells attenuate viral myocarditis in murine model. Cell Transplant 2002;11:753–8.
[15] Di Nicola M, Carlo-Stella C, Magni M, Milanesi M, Longoni PD, Matteucci P, et al. Human bone marrow stromal cells suppress T-lymphocyte proliferation induced by cellular or nonspecific mitogenic stimuli. Blood 2002;99: 3838–43.
[16] Tse WT, Pendleton JD, Beyer WM, Egalka MC, Guinan EC. Suppression of allogeneic T-cell proliferation by human marrow stromal cells: implications in transplantation. Transplantation 2003;75:389–97.
[17] Rollins BJ. Chemokines. Blood 1997;90:909–28.
[18] Fuse K, Kodama M, Hanawa H, Okura Y, Ito M, Shiono T, et al. Enhanced expression and production of monocyte chemoattractant protein-1 in myocarditis. Clin Exp Immunol 2001;124:346–52.
[19] Kolattukudy PE, Quach T, Bergese S, Breckenridge S, Hensley J, Altschuld R, et al. Myocarditis induced by targeted expression of the MCP-1 gene in murine cardiac muscle. Am J Pathol 1998;152:101–11.
[20] Ji JF, He BP, Dheen ST, Tay SS. Interactions of chemokines and chemokine receptors mediate the migration of mesenchymal stem cells to the impaired site in the brain after hypoglossal nerve injury. Stem Cells 2004;22:415–27.
[21] Wang L, Li Y, Chen J, Gautam SC, Zhang Z, Lu M, et al. Ischemic cerebral tissue and MCP-1 enhance rat bone marrow stromal cell migration in interface culture. Exp Hematol 2002;30:831–6.
[22] Damas JK, Eiken HG, Oie E, Bjerkeli V, Yndestad A, Ueland T, et al. Myocardial expression of CC- and CXC-chemokines and their receptors in human end-stage heart failure. Cardiovasc Res 2000;47:778–87.
[23] Damas JK, Aukrust P, Ueland T, Odegaard A, Eiken HG, Gullestad L, et al. Monocyte chemoattractant protein-1 enhances and interleukin-10 suppresses the production of inflammatory cytokines in adult rat cardiomyocytes. Basic Res Cardiol 2001;96:345–52.
[24] Ing DJ, Zang J, Dzau VJ, Webster KA, Bishopric NH. Modulation of cytokine-induced cardiac myocyte apoptosis by nitric oxide, Bak, and Bcl-x. Circ Res 1999;84:21–33.
[25] Hirota H, Chen J, Betz UA, Rajewsky K, Gu Y, Ross Jr J, et al. Loss of a gp130 cardiac muscle cell survival pathway is a critical event in the onset of heart failure during biomechanical stress. Cell 1999;97: 189–98.
[26] Gnecchi M, He H, Liang OD, Melo LG, Morello F, Mu H, et al. Paracrine action accounts for marked protection of ischemic heart by Akt-modified mesenchymal stem cells. Nat Med 2005;11:367–8.
[27] Lee JK, Zaidi SH, Liu P, Dawood F, Cheah AY, Wen WH, et al. A serine elastase inhibitor reduces inflammation and fibrosis and preserves cardiac function after experimentally-induced murine myocarditis. Nat Med 1998;4:1383–91.
[28] Ono K, Matsumori A, Shioi T, Furukawa Y, Sasayama S. Contribution of endothelin-1 to myocardial injury in a murine model of myocarditis: acute effects of bosentan, an endothelin receptor antagonist. Circulation 1999;100:1823–9.

Available online at www.sciencedirect.com
ScienceDirect
Biochemical and Biophysical Research Communications 349 (2006) 1242–1249
BBRC
www.elsevier.com/locate/ybbrc

Beraprost sodium enhances neovascularization in ischemic myocardium by mobilizing bone marrow cells in rats

Yoshinori Miyahara [a], Shunsuke Ohnishi [a], Hiroaki Obata [a], Kozo Ishino [b], Shunji Sano [b], Hidezo Mori [c], Kenji Kangawa [d], Soichiro Kitamura [e], Noritoshi Nagaya [a,*]

[a] *Department of Regenerative Medicine and Tissue Engineering, National Cardiovascular Center Research Institute, Osaka, Japan*
[b] *Department of Cardiovascular Surgery, Okayama University Graduate School of Medicine, Dentistry and Pharmaceutical Sciences, Okayama, Japan*
[c] *Department of Cardiac Physiology, National Cardiovascular Center Research Institute, Osaka, Japan*
[d] *Department of Biochemistry, National Cardiovascular Center Research Institute, Osaka, Japan*
[e] *Department of Cardiovascular Surgery, National Cardiovascular Center, Osaka, Japan*

Received 13 August 2006
Available online 7 September 2006

Abstract

Beraprost sodium, an orally active prostacyclin analogue, has vasoprotective effects such as vasodilation and antiplatelet activities. We investigated the therapeutic potential of beraprost for myocardial ischemia. Immediately after coronary ligation of Sprague–Dawley rats, beraprost (200 μg/kg/day) or saline was subcutaneously administered for 28 days. Four weeks after coronary ligation, administration of beraprost increased capillary density in ischemic myocardium, decreased infarct size, and improved cardiac function in rats with myocardial infarction. Beraprost markedly increased the number of CD34-positive cells and c-kit-positive cells in plasma. Also, four weeks after coronary ligation of chimeric rats with GFP-expressing bone marrow, bone marrow-derived cells were incorporated into the infarcted region and its border zone. Treatment with beraprost increased the number of GFP/von Willebrand factor-double-positive cells in the ischemic myocardium. These results suggest that beraprost has beneficial effects on ischemic myocardium partly by its ability to enhance neovascularization in ischemic myocardium by mobilizing bone marrow cells.

Keywords: Prostacyclin analogue; Myocardial infarction; Neovascularization; Bone marrow mobilization

Interruption of myocardial blood flow leads to rapid death of cardiomyocytes and vascular structures, resulting in the development of heart failure [1]. Stem or progenitor cells are mobilized from bone marrow into the peripheral blood in response to tissue ischemia, migrate to sites of injured tissues, and differentiate into endothelial cells and cardiomyocytes [2–4]. However, the compensatory mechanisms are insufficient to heal infarcted myocardium. Earlier studies have shown that bone marrow cells artificially mobilized by cytokines repair the infarcted heart and improve cardiac function after acute myocardial infarction [5,6]. Therefore, enhancement of bone marrow cell mobilization leading to neovascularization following revascularization would be beneficial for the treatment of acute myocardial infarction.

Beraprost sodium (BPS) is a chemically stable prostacyclin analogue owing to its cyclo-pentabenzofuranyl structure [7]. It has been well established that BPS has vasoprotective effects such as vasodilation and antiplatelet activities [8–11]. Thus, BPS has been used in the treatment of peripheral arterial disease [12,13] and pulmonary arterial hypertension [14,15]. Although a limited number of studies suggest therapeutic potential of prostacyclin for the treatment of myocardial ischemia [16–18], the underlying mechanisms still remain unclear. In addition, little information is available regarding the therapeutic potential of prostacyclin analogues such as BPS for myocardial ischemia. A recent study has shown that BPS activates endothelial

* Corresponding author. Fax: +81 6 6833 9865.
E-mail address: nnagaya@ri.ncvc.go.jp (N. Nagaya).

0006-291X/$ - see front matter © 2006 Elsevier Inc. All rights reserved.
doi:10.1016/j.bbrc.2006.08.178

nitric oxide synthase (eNOS) through the c-AMP/protein kinase A pathway [19]. Activation of eNOS is known to contribute to bone marrow cell mobilization, leading to neovascularization [20]. These results raise the possibility that BPS may have beneficial effects on the ischemic myocardium through enhancement of bone marrow cell mobilization.

Thus, the purposes of this study were: (1) to examine the effect of BPS on mobilization and recruitment of bone marrow cells after acute myocardial infarction, (2) to investigate whether BPS induces neovascularization in the ischemic myocardium, and (3) to investigate whether treatment with BPS improves cardiac function in rats with myocardial infarction.

Methods

Model of myocardial infarction. We used male Sprague–Dawley rats (Japan SLC Inc., Hamamatsu, Japan) weighing 185–215 g. Myocardial infarction was produced by left coronary ligation, as described previously [21]. Briefly, after rats were anesthetized with sodium pentobarbital (30 mg/kg), they were artificially ventilated with a volume-regulated respirator. The heart was exposed via a left thoracotomy incision. Then, the left coronary artery was ligated 2–3 mm from its origin between the pulmonary artery conus and the left atrium with a 6-0 Prolene suture. Finally, the heart was restored to its normal position, and the chest was closed. Experimental protocols were performed in accordance with the "Guidelines of the Animal Care Ethics Committee of the National Cardiovascular Center Research Institute", which complies NIH Guidelines.

Administration of BPS. Immediately after coronary ligation, BPS (200 μg/kg/day, Astellas Pharma Inc., Tokyo, Japan) was subcutaneously administered to surviving rats using an osmotic mini-pump for 4 weeks (BPS group, $n = 12$). As a control, saline was similarly administered to rats receiving coronary ligation (Control group, $n = 12$).

Echocardiographic studies. Echocardiographic studies were performed 4 weeks after coronary ligation. M-mode tracings were obtained at the level of the papillary muscles using an echocardiographic system equipped with a 7.5-MHz phased-array transducer (HP SONOS 5500; Hewlett Packard Co., Andover, MA). Anterior and posterior end-diastolic and end-systolic wall thickness, LV end-diastolic and end-systolic dimensions, and LV fractional shortening were measured by the American Society for Echocardiography leading-edge method in three consecutive cardiac cycles. LV meridional wall stress was estimated as $0.344 \times \text{LV pressure} \times \{\text{LV dimension}/(1 + \text{PWT/LV dimension})\}$, where PWT is posterior wall thickness [22].

Hemodynamic studies. Hemodynamic studies were performed 4 weeks after coronary ligation, following echocardiography. After anesthesia with pentobarbital sodium, a 1.5F micromanometer-tipped catheter (Millar Instruments Inc., Houston, TX) was advanced into the LV through the right common carotid artery. Hemodynamic variables were measured with a pressure transducer connected to a polygraph. After completion of these measurements, the left and right ventricles and the lungs were excised and weighed. Infarct size was determined as a percentage of the entire LV area ($n = 5$ in each group), as reported previously [23]. Briefly, incisions were made in the posterior LV so that the tissue could be pressed flat. The circumference of the entire flat LV and of the visualized infarcted area, as judged from both the epicardial and endocardial sides, was outlined on a clear plastic sheet. The difference in weight between the two marked areas on the sheet was used to determine infarct size and was expressed as a percentage of LV surface area.

Measurement of plasma ANP level. Blood samples were obtained 4 weeks after coronary ligation. Plasma atrial natriuretic peptide (ANP), a marker for heart failure, was measured by enzyme immunoassay (Peninsula Laboratories Inc., San Carlos, CA).

Mononuclear cell mobilization and FACS analysis. To investigate whether administration of BPS mobilizes bone marrow cells, an additional 12 rats were randomized to receive BPS (200 μg/kg/day, BPS group, $n = 6$) or saline (Control group, $n = 6$). On the third day of BPS or saline treatment, 4 ml of blood was drawn from the inferior vena cava of each rat. Peripheral blood was obtained at the end of infusion. After mononuclear cells were counted, they were incubated for 30 min at 4 °C with fluorescein isothiocyanate (FITC)-conjugated mouse monoclonal antibodies against rat CD34 (clone ICO-115, Santa Cruz) and CD45 (clone OX-1), and FITC-conjugated rabbit anti-rat c-Kit polyclonal antibody (clone C-19, Santa Cruz). Immunofluorescence-labeled cells were analyzed by quantitative flow cytometry with a FACSCalibur flow cytometer (BD Biosciences, Mountain View, CA). Isotype-identical antibodies served as controls.

RT-PCR assay. To investigate whether bone marrow cells express the prostacyclin receptor (IP receptor), we analyzed expression of its mRNA by reverse transcription-polymerase chain reaction (RT-PCR). In brief, total RNA of bone marrow cells was extracted with guanidine isothiocyanate (RNeasy Mini Kit, Qiagen). Then, reverse-transcribed single-stranded cDNA was subjected to PCR (PCR Amplification Kit, Takara) using primer sets for the IP receptor (Hokkaido System Science Co., Ltd., Sapporo, Japan, forward, 5′-GGCACGAGAGGATGAAGTTTACC-3′; reverse, 5′-GTCAGAGGCACAGCAGTCAATGG-3′) and G3PDH (Clonetech Laboratories Inc., Mountain View, CA, forward, 5′-TG AAGGTCGGTGTCAACGGATTTGGC-3′; reverse, 5′-CATGTAGG CCATGAGGTCCACCAC-3′).

Creation of bone marrow-chimeric rats. To assess recruitment of bone marrow cells after BPS administration, bone marrow transplantation was performed by using male normal Sprague–Dawley rats as recipients and male Green fluorescent protein (GFP)-transgenic rats (SD-Tg [Act-EGFP] CZ-004Osb, Japan SLC Inc.) as donors, using a previously described method [24]. Briefly, bone marrow was harvested by flushing the cavity of femurs and tibias from GFP-transgenic rats with phosphate-buffered saline. Then, 3×10^7 GFP-positive bone marrow cells were individually administered to 12 lethally irradiated (900c Gray) rats via the tail vein. Four weeks after transplantation, flowcytometric analysis determined that 90% of peripheral blood mononuclear cells from both donors and 8 of 12 chimeric rats were GFP-positive, suggesting the establishment of stable chimerism. These chimeric rats were subjected to left coronary ligation, followed by administration of BPS (200 μg/kg/day, BPS group, $n = 4$) or saline (Control group, $n = 4$) using an osmotic mini-pump for 4 weeks.

Histological examination. To detect fibrosis in the cardiac muscle, the LV myocardium ($n = 5$, each group) was fixed in 10% formalin, cut transversely in three sections, embedded in paraffin, and stained with Masson's trichrome. To detect capillary endothelial cells in the peri-infarct area, we performed DAB staining (LSAB2 System HRP, Dako Cytomation Co., Denmark) using rabbit polyclonal anti-von Willebrand factor (vWF) antibody (Dako). A total of 10 different fields from three different sections were randomly selected, and the number of capillaries was counted in the peri-infarct area using a light microscope at 200× magnification. Capillary density was expressed as the mean number of capillaries per square millimeter. Also, 4 weeks after coronary ligation in bone marrow-chimeric rats ($n = 4$ in each group), the LV myocardium was excised, embedded in OCT compound, snap-frozen in liquid nitrogen, and cut transversely into 6-μm-thick sections from base to apex. Immunofluorescent staining was performed using rabbit polyclonal anti-vWF antibody (Dako), mouse monoclonal anti-cardiac troponin T antibody (Neomarkers, Fremont, CA), and rabbit polyclonal Alexa 488-conjugated anti-GFP antibody (Molecular Probes Inc., Eugene, OR). The nuclei were counterstained with 4′,6′-diamidino-2-phenylindole (DAPI). We measured the number of GFP/vWF-double-positive cells incorporated into vascular structures in 10 randomly selected fields in the peri-infarct area per section in a blinded fashion using a fluorescence microscope.

Statistical analysis. Numerical values are expressed as means ± SEM. Comparisons of parameters between two groups were made by unpaired Student's t test. A value of $p < 0.05$ was considered significant.

Results

Cardiac structure

Body weight at 4 weeks after coronary ligation was significantly greater in the BPS group than in the Control group (Table 1). Right ventricular weight and lung weight in the BPS group were significantly smaller than those in the Control group, although LV weight did not differ between the two groups. Moderate to large infarcts were observed in the Control group (Fig. 1A). However, administration of BPS significantly decreased infarct size in rats with myocardial infarction (Fig. 1A and B). BPS significantly decreased LV end-diastolic dimension (LVDD) (Fig. 1C).

Table 1
Physiological profiles of experimental groups

	Control	BPS
Number	12	12
Body weight (g)		
Baseline	198 ± 3	204 ± 3
After treatment	319 ± 6	352 ± 9*
LV wt/body wt (g/kg)	2.28 ± 0.04	2.27 ± 0.04
RV wt/body wt (g/kg)	0.99 ± 0.05	0.61 ± 0.02**
Lung wt/body wt (g/kg)	6.55 ± 0.62	3.88 ± 0.1**
Plasma AND level (pg/ml)	798 ± 99	498 ± 57*

Control, infarct rats without treatment; BPS, infarct rats treated with BPS administration; AND, atrial natriuretic protein. Data are expressed as means ± SEM. $^{*}p < 0.05$, $^{**}p < 0.01$ vs. Control group.

Cardiac function

Neither heart rate nor mean arterial pressure differed between the BPS and Control groups (Table 2). LV fractional shortening and LV maximum dP/dt in the BPS group were significantly greater than those in the Control group (Fig. 2A and B). LV end-diastolic pressure (LVEDP) in the BPS group was significantly lower than that in the Control group (Fig. 2C). LV minimum dP/dt was also improved by BPS (Fig. 2D). Treatment with BPS attenuated the increase in plasma ANP level after myocardial infarction (Table 1). BPS significantly increased anterior wall thickening, although it did not significantly alter posterior wall thickening (Table 2). Thickness of the anterior and posterior walls tended to be greater in the BPS group, but these changes did not reach statistical significance. LV diastolic wall stress in the BPS group was significantly lower than that in the Control group.

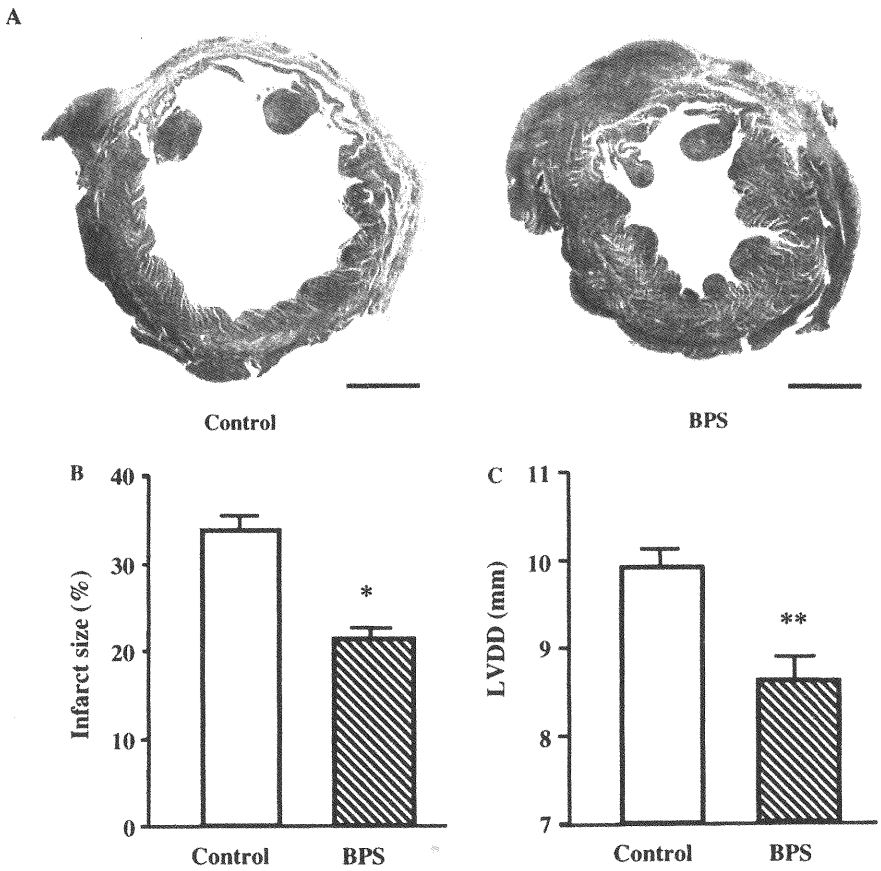

Fig. 1. (A) Representative examples of Masson's trichrome staining of transverse sections of LV myocardium 4 weeks after coronary ligation. Scale bars = 2 mm. (B,C) Quantitative analysis of infarct size and LV end-diastolic dimension (LVDD). Infarcted area and LVDD in the BPS group were significantly smaller than those in the Control group. Data are expressed as means ± SEM. $^{*}p < 0.05$, $^{**}p < 0.01$ vs. Control group.

Table 2
Echocardiographic and hemodynamic data

	Control	BPS
AWT diastole (mm)	0.62 ± 0.04	0.74 ± 0.05
AW thickening (%)	17 ± 3	34 ± 6*
PWT diastole (mm)	1.55 ± 0.07	1.70 ± 0.04
PW thickening (%)	43 ± 4	49 ± 3
Heart rate (bpm)	458 ± 7	471 ± 10
Mean arterial pressure (mmHg)	103 ± 5	115 ± 4
LV systolic pressure (mmHg)	113 ± 4	127 ± 5*
LV diastolic wall stress (kdyne/cm^2)	24 ± 4	5 ± 1**
LV systolic wall stress (kdyne/cm^2)	267 ± 18	225 ± 14

AWT, anterior wall thickness; AW, anterior wall; PWT, posterior wall thickness; PW, posterior wall. Data are expressed as means ± SEM. *$p < 0.05$, **$p < 0.01$ vs. Control group.

Mobilization of bone marrow cells

RT-PCR demonstrated that IP receptor mRNA was expressed in bone marrow cells (Fig. 3A), indicating a direct effect of BPS on these cells. Three-day administration of BPS significantly increased the number of peripheral blood mononuclear cells compared to saline administration (Fig. 3B). Administration of BPS markedly increased the number of circulating progenitor cells such as CD34-positive cells and c-kit-positive cells (Fig. 3C and D). BPS also increased the number of CD45-positive hematopoietic lineage cells (Fig. 3E).

BPS-induced neovascularization

Chimeric rats with GFP-expressing bone marrow were used to assess recruitment of bone marrow cells. Four weeks after coronary ligation, bone marrow-derived GFP-positive cells were incorporated predominantly into the infarcted region and its border zone (Fig. 4A), while these cells were rarely detected in the noninfarcted myocardium. Some of the GFP-positive cells stained for vWF and formed vascular structures. Semi-quantitative analysis demonstrated that the number of GFP-positive cells in the myocardium was significantly greater in the BPS group than in the Control group (Fig. 4B). The number of GFP-vWF double-positive cells (bone marrow-derived endothelial cells) in the ischemic myocardium was significantly greater in the BPS group than in the Control group (Fig. 4C). In addition, a small number of GFP-troponin T-double-positive cells were observed in the BPS group (Fig. 4D).

Capillary density

In the peri-infarct area, clustering of relatively small vessels was seen in BPS-treated hearts, which is indicative of recent endothelial regeneration (Fig. 5A). Semi-quantitative analysis also demonstrated that administration of BPS significantly increased the capillary density in the peri-infarct area compared to the Control group (Fig. 5B).

Discussion

In the present study, we demonstrated that treatment with BPS (1) decreased infarct size and improved cardiac structure and function in rats with acute myocardial infarction, (2) increased the number of circulating progenitor cells such as CD34-positive cells and c-kit-positive cells in rats, and (3) increased the number of bone marrow-derived endothelial cells and the capillary density in the ischemic myocardium. These results suggest that BPS may have beneficial effects on ischemic myocardium at least in part through enhancement of neovascularization by mobilizing bone marrow cells.

Earlier studies have reported that prostacyclin has cardioprotective effects in ischemia–reperfusion injury through inhibition of neutrophil activation and migration [25,26]. BPS is also reported to inhibit chemotaxis and superoxide anion production of neutrophils which contribute to tissue damage by releasing tissue destructive lysosomal enzymes [27]. Infusion of BPS has been shown to reduce infarct size in the dog heart with left coronary occlusion by reducing myocardial oxygen demand and by inhibition of the migration of neutrophils [28]. However, these

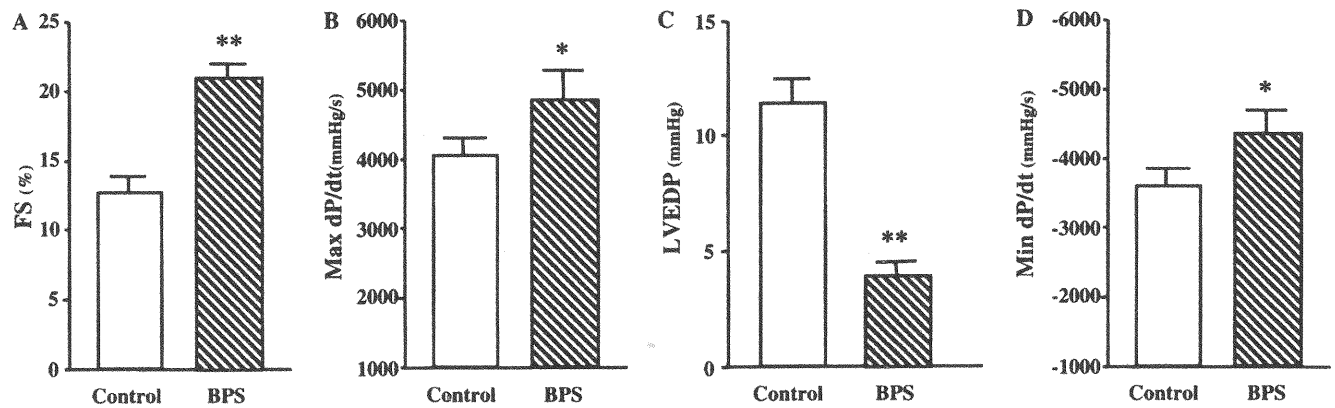

Fig. 2. Cardioprotective effects of BPS on echocardiographic and hemodynamic parameters. FS, fractional shortening; LVEDP, LV end-diastolic pressure; Max and Min dP/dt, maximum and minimum dP/dt. Data are expressed as means ± SEM. *$p < 0.05$, **$p < 0.01$ vs. Control group.